

# Global estimate of aerosol direct radiative forcing from satellite measurements

Nicolas Bellouin<sup>1,2</sup>, Olivier Boucher<sup>1</sup>, Jim Haywood<sup>2</sup>, and M. S. Reddy<sup>1,3</sup>

<sup>1</sup> *Laboratoire d'Optique Atmosphérique, Université des Sciences et Technologies de Lille / CNRS, Lille, France*

<sup>2</sup> *United Kingdom Met Office, Exeter, United Kingdom*

<sup>3</sup> *[NOAA](#)/Geophysical Fluid Dynamics Laboratory, Princeton University, USA*

The direct effect of atmospheric aerosols consists of scattering and absorption of incoming solar radiation. Through this process, anthropogenic aerosols exert a direct radiative forcing (DRF) of the climate system<sup>1</sup>. So far DRF estimates are derived from global models which incorporate a representation of the aerosol cycles<sup>1-3</sup>. Although models are compared and validated against observations, their estimates of aerosol DRF remain uncertain. Previous estimates of the aerosol direct effect from satellite measurements had limited information on aerosol type and were limited to oceans only<sup>4-5</sup>. Here we use the state-of-the-art MODIS aerosol retrievals<sup>6-7</sup> combined with TOMS<sup>8</sup> and SSM/I<sup>9</sup> measurements to estimate the clear-sky DRF for the year 2002. For the first time, aerosol DRF can be estimated by aerosol type both over ocean and land. Anthropogenic aerosols are shown to increase the outgoing shortwave flux by  $2.7 \text{ Wm}^{-2}$  at the top of the atmosphere, in clear-sky on a global, annual average. The clear-sky part of the total DRF is  $-x.x \text{ Wm}^{-2}$  and is used to constrain the IPCC<sup>1</sup> estimates and climate models of intermediate complexity<sup>10</sup>.

Atmospheric aerosols may be grouped into four generic types: Mineral dust, marine aerosol, biomass burning aerosol and industrial pollution. The first two types are of natural origin, while the last two types are primarily emitted from human agricultural and industrial activities although some mineral dust emissions can also be due to human-induced desertification and some biomass burning aerosol emissions are due to large-scale fires of natural origin in boreal regions such as Siberia and Canada. Nevertheless, the majority of anthropogenic aerosols of climatic importance consist of particles smaller than  $1\text{ }\mu\text{m}$ , also called accumulation-mode particles. In contrast, natural aerosols exhibit a larger contribution of large particles. Also, each aerosol type has its own absorption properties. In the shortwave, mineral dust and marine aerosols are weakly absorbing, whereas anthropogenic aerosols exhibit a moderate to strong absorption, depending on aerosol type which can be related to the location of its sources. Moreover mineral dust and biomass-burning aerosols are absorbing in the ultraviolet.

The Moderate Resolution Imaging Spectrometer (MODIS) space instrument has operated onboard the Terra and Aqua platforms since December 1999 and May 2002, respectively. This instrument has 36 narrow channels ranging from the UV to the IR spectrum, but only the visible and near-IR channels are used for aerosol studies. Here, we use the retrievals of two aerosol optical properties at  $0.55\text{ }\mu\text{m}$ <sup>6-7</sup>; the total aerosol optical thickness (AOT), which measures the column aerosol extinction, and the accumulation-mode fraction, which gives the fraction of the total AOT being due to particles with a radius smaller than  $1\text{ }\mu\text{m}$ . These quantities are available for clear sky conditions over oceans and land surfaces, except deserts and snow-covered regions, where the surface contribution to the measured signal is too large for accurate

retrievals. This limitation means that most mineral dust events are not detected over land. Retrievals from MODIS have been successfully validated against ground-based measurements<sup>11-12</sup>, although it has been shown that retrievals are less accurate over land than over the ocean. Specifically, the accumulation-mode fraction is not reliable over land surfaces. This study uses data from the Terra platform for the year 2002, when calibration of the instrument is stable. Other sources of data include the TOMS (Total Ozone Mapping Spectrometer) aerosol index<sup>8</sup>, which is a semi-quantitative retrieval of UV-absorbing aerosol loading, and surface wind speeds from SSM/I (Special Sensor Microwave Imager<sup>9</sup>), allowing an estimate of the marine AOT<sup>13</sup>.

Two steps are needed to get the component aerosol DRF. First, we split the MODIS total AOT into optical thicknesses for the four generic aerosol types. Then we estimate the DRF using single scattering optical properties (especially absorption) of the identified aerosol type (see the Methods section). Figure 1 shows the annual distributions of optical thickness for mineral dust, marine aerosol, and anthropogenic aerosols for 2002. The total optical thickness is also presented. The capacity of the algorithm to identify a given aerosol type is well represented by these distributions. As expected, mineral dust is the main contributor to the aerosol loading off the coasts of Western Africa and in the Persian Gulf. The algorithm also detects seasonal events originating from Australia and China. Areas of high AOT of marine aerosol are well identified as such. Anthropogenic aerosols, which are the only aerosols defined over land, are shown to be significant contributors to the total AOT over oceanic areas downwind of major biomass burning events in Central and Southern Africa, and off the coasts of North America, Europe, China, and India. Seasonal distributions (not shown) are consistent with our existing knowledge of aerosol sources and transport.

The globally-averaged component optical thicknesses and direct radiative effects are given in Table 1. We focus now on anthropogenic aerosols, composed of biomass-burning and industrial aerosols, and examine their contribution to climate change in terms of DRF. On a global average for clear-sky conditions, anthropogenic aerosols reflect an additional  $2.7 \text{ Wm}^{-2}$  of solar radiation back to space and reduce the solar flux at the surface by  $6.0 \text{ Wm}^{-2}$ . The difference between these two quantities corresponds to the energy absorbed in the aerosol layer, which amounts to  $3.3 \text{ Wm}^{-2}$ . Most of the aerosol DRF is over land, which implies that significant efforts need to be made in order to improve satellite retrievals over land surfaces. As we supply different optical properties depending on the location, we are able to quantify the contributions of different regions to the AOT and radiative effects. Weakly absorbing aerosols around Europe, Far-East Asia and North America contribute to 44% of the anthropogenic AOT and 53% of the top-of-atmosphere DRF. Biomass-burning aerosols originating from Africa and South America represent 34% of the anthropogenic AOT, but their strong absorption increases their contribution to the atmospheric (or absorption) DRF to 45%.

We can further analyse our results in light of model simulations. The LMD-ZT general circulation model<sup>2</sup> is run in nudged mode for the year 2002 and daily aerosol fields are sampled according to the MODIS clear-sky retrievals. With an annually-averaged AOT of 0.007 for the marine aerosol over land, the model confirms our assumption that we can neglect this contribution. Over ocean, the marine AOT is smaller in the model (0.032) than it is in the MODIS measurements (0.101). These discrepancies may be due to a bias towards higher AOTs due to surface reflectance or cirrus contamination in the MODIS retrievals and/or to inaccuracies in the model parameterisations. In the model the dust AOT is about 6 times larger over land than over ocean (0.061 and 0.010, respectively) but only 3 times larger (0.035 and 0.012,

respectively) if we exclude cloudy sky conditions and regions of bright surfaces as done in MODIS retrievals. This amounts to a dust AOT over land of 0.045 if we apply the same ratio to MODIS data. The model also indicates an AOT of natural origin of 0.025 over land, beyond the dust contribution. The MODIS AOT over land is therefore an upper limit of the anthropogenic AOT and our model results indicate that the overestimation is of the order of 0.07 or 28%. Over ocean, our MODIS estimate is a lower limit for the anthropogenic AOT as the marine component may contain some dust and anthropogenic contributions.

We can approximate the total (or all-sky) DRF,  $DRF_{total}$ , by assuming that the cloudy-sky contribution is negligible so that  $DRF_{total}$  is simply the clear-sky DRF (estimated above to be  $-2.7 \text{ Wm}^{-2}$ ) multiplied by the clear-sky fraction (or one minus the cloud fraction). Using the MODIS cloud fraction<sup>14</sup>, our results suggest  $DRF_{total} = -x.x \text{ Wm}^{-2}$ . In fact, the cloudy sky contribution is likely to be either negligible for scattering aerosols or positive for absorbing aerosols above cloud<sup>15</sup> (but cannot be estimated from satellite remote-sensing without the knowledge of the aerosol and cloud vertical profiles). The fact that the contribution to the total DRF from aerosols residing above cloud may be positive leads us to believe that our estimate of  $DRF_{total}$  is an effective lower bound of the all-sky aerosol DRF (i.e., the most negative possible DRF). This is supported by the fact that our algorithm includes every aerosol, regardless of its origin, in the anthropogenic AOT over land, and that MODIS retrievals may suffer a degree of cirrus and sea foam contamination, leading to erroneously large AOT in some areas. The radiative transfer calculations use a well-validated radiative transfer code<sup>16</sup>, with a good representation of the land surface albedo<sup>17</sup>, and are not expected to introduce a significant uncertainty on  $DRF_{total}$ . It can then be used as a realistic constraint for the modelled estimates of the aerosol DRF. The IPCC third assessment report<sup>1</sup> estimates this forcing to be  $-0.4$ ,  $-0.1$ ,  $+0.2$ , and  $-$

0.2 Wm<sup>-2</sup> for sulphate aerosol, fossil-fuel organic carbon, fossil-fuel black carbon, and biomass-burning aerosols, respectively. Each of these values has an associated uncertainty, and the total aerosol DRF can be estimated using probability density functions<sup>10,18</sup> (PDFs).

The estimate of the lower bound of DRF<sub>total</sub>, -x.x Wm<sup>-2</sup>, is compared against those derived from model estimates by using log-normal distributions for the PDFs of each of the individual modelled radiative forcing components listed above<sup>18</sup>. The PDF approach reveals that a modelled radiative forcing more negative than -x.x Wm<sup>-2</sup> occurs with a 39%, 24%, and 14% probability for standard deviations of 1, 1.5 and 2 encompassing the uncertainty range (Figure 2). Because our results provide an effective *lower bound* for DRF<sub>total</sub> this suggests a substantial degree of inconsistency between the model estimates and those derived independently from our satellite observations; either the mean DRF from the models is too strongly negative, or the uncertainty associated with the modelling efforts is too large. The implication is that extreme negative values for the direct radiative forcing due to anthropogenic aerosols are unlikely, with important consequences for climate modelling studies such as those investigating climate sensitivity, and detection and attribution of climate change.

## Methods

The algorithm has two independent parts: the first one estimates the optical thickness of mineral dust, marine aerosol, and anthropogenic aerosols, while the second one relies on radiative transfer calculations to convert these AOTs into DRFs at the top of

the atmosphere and at the surface. The algorithm uses daily values of MODIS retrievals at the  $1^\circ \times 1^\circ$  resolution<sup>6-7</sup>.

### **Component optical thicknesses over ocean.**

The range of possible values (from 0 to 1) for the accumulation-mode fraction,  $f_{acc}$ , is divided into three intervals. For pixels where  $f_{acc}$  is smaller than 0.5, the aerosol is likely to be mineral dust, marine aerosol or a mixture of those two. Dust presence is detected using the monthly-averaged TOMS aerosol index<sup>8</sup>. Daily values cannot be used, as MODIS and TOMS overpass times and clear-sky detection algorithms are not comparable. If the TOMS aerosol index is larger than 1.0, mineral dust is identified, while a part of the optical thickness is attributed to marine aerosol, as a function of SSM/I daily surface wind speed<sup>9,13</sup>. If the TOMS aerosol index is smaller than 1.0, the total optical thickness is attributed to marine aerosol. Pixels where  $f_{acc}$  is between 0.5 and 0.7 can correspond to mineral dust, marine aerosol, anthropogenic aerosols and a mixture of these three. Again, the TOMS aerosol index informs about the presence of at least one UV-absorbing aerosol. In this case, after removing a background marine optical thickness based on wind speed, the accumulation-mode part of the optical thickness is attributed to anthropogenic aerosols while the coarse-mode AOT is attributed to mineral dust. Finally, when  $f_{acc}$  is larger than 0.7, which is a fraction achievable only by anthropogenic aerosol, the total optical thickness, corrected for the marine background, is attributed to anthropogenic aerosols.

### **Component optical thicknesses over land.**

As mentioned above  $f_{acc}$  is not a reliable parameter over land. Since marine aerosol is not significant over land, and desert areas are not considered in MODIS retrievals (due to the brightness of this type of surface), we assume that the optical thickness is representative of anthropogenic aerosols only. However, south of the Sahara, some

transported mineral dust can be misidentified as anthropogenic aerosols. This is further discussed in the main text.

### **Component direct radiative forcing.**

Aerosol radiative properties are derived from ground-based measurements at selected sites of the Aerosol Robotic Network (AERONET) following the work of Dubovik *et al.*<sup>19</sup> and Bellouin *et al.*<sup>4</sup>. Mineral dust properties are those measured at the Cape-Verde site. Marine aerosol properties are taken from analysis of the Hawaii site measurements, but the single-scattering albedo is increased to 0.99 at 0.55  $\mu\text{m}$  as it is believed that the absorption measured in Hawaii is due to local pollution sources. For anthropogenic aerosols, the optical thickness is derived in a consistent way globally, but when optical properties are considered, they have to be representative of the local aerosol. Therefore we divided the world into six regions (industrial pollution in North America and Eurasia, biomass-burning in South-America and Africa, mixture of pollution and biomass-burning in Central America and India). Aerosol properties are determined from one or several AERONET sites representative of this region. Over ocean, the surface albedo<sup>20</sup> depends on the solar zenith angle and is calculated for a wind speed of 7  $\text{ms}^{-1}$ . Over land, the surface albedo is computed from MODIS retrievals of the albedo for direct and diffuse radiation, with a different albedo in the visible and in the near-infrared spectra<sup>17</sup>. Surface albedo is adjusted for the effect of the identified aerosol on radiative fluxes. Radiative transfer calculations are performed using a discrete-ordinate solver<sup>16</sup>, with 24 shortwave wavebands and 24 streams. The 24 hour-averaged DRF is computed by integrating the instantaneous radiative forcing over the solar zenith angles as a function of latitude and season. Averages are weighted by the fraction of clear sky in a  $1^\circ \times 1^\circ$  pixel (also termed pixel counts).



Figure 1: Distributions of the aerosol optical thickness at  $0.55\ \mu\text{m}$  for the year 2002 for the total aerosol and by component (mineral dust, marine aerosol, and biomass and pollution aerosol).

Figure 2: Probability density functions of the aerosol direct radiative forcing from the IPCC estimates. The lower bound implied by this study is shown by a vertical bar.

Figure 1: Distributions of the aerosol optical thickness at  $0.55\ \mu\text{m}$  for the year 2002 for the total aerosol and by component (mineral dust, marine aerosol, and biomass and pollution aerosol).

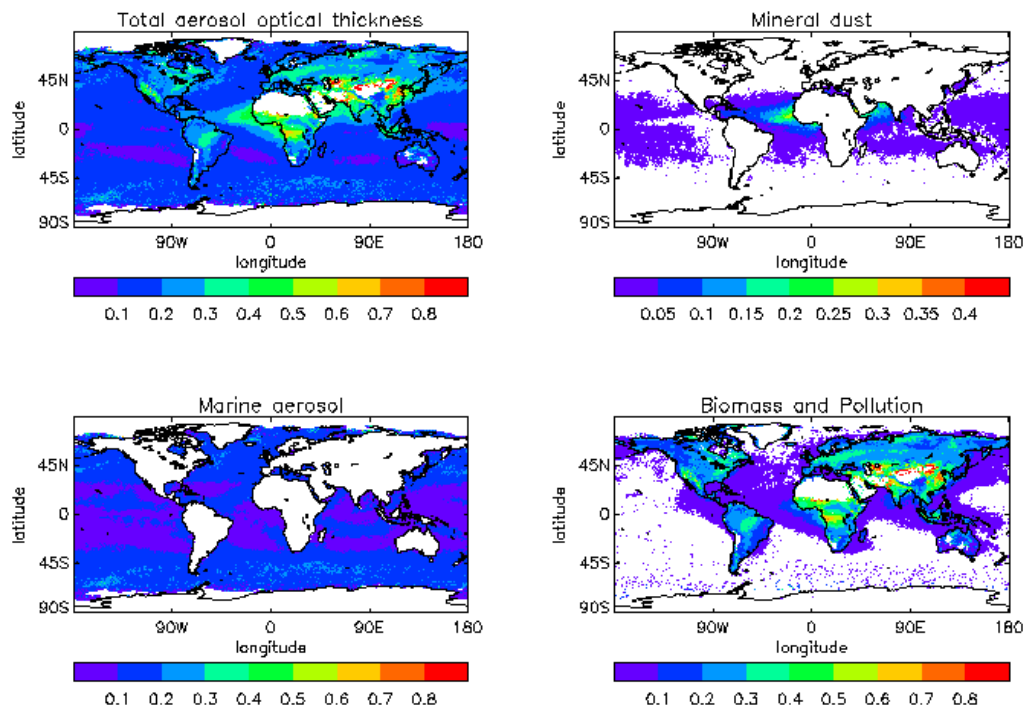
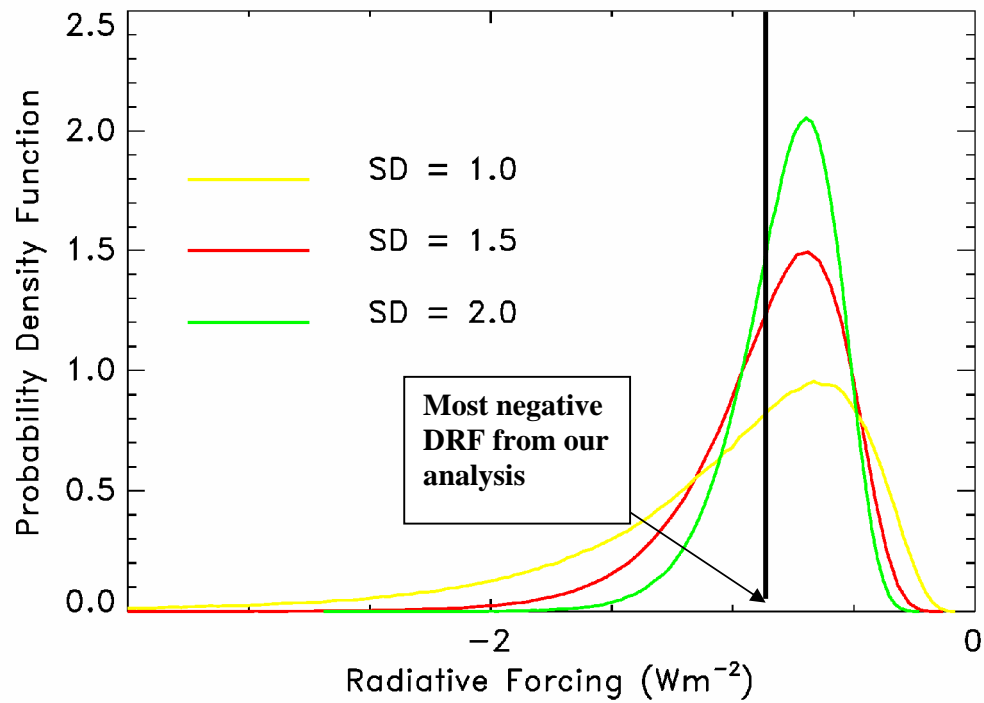


Figure 2: Probability density functions of the aerosol direct radiative forcing from the IPCC estimates. The lower bound implied by this study is shown by a vertical bar.



**Table 1: Global averages for the year 2002.**

Aerosol optical thickness at 0.55 $\mu\text{m}$				
		Global	Ocean	Land
All aerosols		0.177	0.140	0.248
Marine aerosol		0.067	0.101	0.000
Mineral dust		0.010	0.015	0.000
Anthropogenic aerosols		0.100	0.024	0.248
Aerosol shortwave direct radiative forcings from observations ( $\text{Wm}^{-2}$ )				
		Global	Ocean	Land
Marine aerosol	Top of atmo.	-3.4	-5.1	
	Surface	-4.0	-6.0	
	Atmospheric (Absorption)	0.6	0.9	
Mineral dust	Top of atmo.	-0.5	-0.8	
	Surface	-0.6	-1.0	
	Atmospheric (Absorption)	0.1	0.2	
Anthropogenic aerosols	Top of atmo.	-2.7	-0.9	-6.0
	Surface	-6.0	-2.0	-13.6
	Atmospheric (Absorption)	3.3	1.1	7.6

## References

1. Ramaswamy, V. *et al.* (eds) *Climate Change 2001: The scientific Basis*, Contribution of WGI to the Third Assessment Report of the IPCC (Cambridge University Press, Cambridge, 2001).
2. Reddy, M. S. *et al.* Estimates of global multi-component aerosol optical depth and direct radiative perturbation in the LMDZT General Circulation Model. *J. Geophys. Res.*, in press (2005).
3. Roberts, D.L. & Jones, A. Climate sensitivity to black carbon aerosol from fossil fuel combustion. *J. Geophys. Res.*, **109**, D16202, doi:10.1029/2004JD004676 (2004).
4. Bellouin, N., Boucher, O., Tanré, D. & Dubovik, O. Aerosol absorption over the clear-sky oceans deduced from POLDER-1 and AERONET observations. *Geophys. Res. Lett.*, **30**, 1748, doi:10.1029/2003GL017121 (2003).
5. Christopher, S.A. & Zhang, J. Shortwave aerosol radiative forcing from MODIS and CERES observations over the oceans. *Geophys. Res. Lett.*, **29**, 1859, doi:10.1029/2002GL014803 (2002).
6. Kaufman, Y. J. *et al.* Operational remote sensing of tropospheric aerosol over land from EOS moderate resolution imaging spectroradiometer. *J. Geophys. Res.*, **102**, 17051-17068 (1997).
7. Tanré, D., Kaufman, Y.J., Herman, M. & Mattoo, S. Remote sensing of aerosol properties over oceans using the MODIS/EOS spectral radiances. *J. Geophys. Res.*, **102**, 16971-16988 (1997).
8. Herman, J.R. *et al.* Global distribution of UV-absorbing aerosols from Nimbus 7/TOMS data. *J. Geophys. Res.*, **102**, 16911-16922 (1997).

9. Wentz, F. A well calibrated ocean algorithm for SSM/I. *J. Geophys. Res.*, **102**, 8703-8718 (1997).
10. Knutti, R., Stocker, T.F., Joos, F. & Plattner, G.-K. Constraints on radiative forcing and future climate change from observations and climate model ensembles. *Nature*, **416**, 719-723 (2002).
11. Remer, L.A. *et al.* Validation of MODIS aerosol retrieval over ocean. *Geophys. Res. Lett.*, **29**, doi:10.1029/2001GL013204 (2002).
12. Chu, D. A., *et al.* Validation of MODIS aerosol optical depth retrieval over land. *Geophys. Res. Lett.*, **29**, doi: 10.1029/2001GL013205 (2002).
13. Smirnov, A., Holben, B.N., T.F. Eck, Dubovik, O. & Slutsker, I. Effect of wind speed on columnar aerosol optical properties at Midway Island. *J. Geophys. Res.*, **108**, 4802, doi:10.1029/2003JD003879 (2003).
14. Platnick, S. *et al.* The MODIS cloud products: Algorithms and examples from Terra. *IEEE Trans. Geosci. Remote Sens.*, **41**, 459-473 (2003).
15. Keil, A. & Haywood, J.M. Solar radiative forcing by biomass aerosol particles over marine clouds during SAFARI-2000. *J. Geophys. Res.*, 8467, **108**, doi:10.1029/2002JD002315 (2003).
16. Key, J. R. & Schweiger, A. J. Tools for atmospheric radiative transfer: STREAMER and FLUXNET. *Computers & Geosciences*, **24**, 443-451 (1998)
17. Schaaf, C. B *et al.* First operational BRDF, albedo nadir reflectance products from MODIS, *Remote Sens. Environ.*, **83**, 135-148 (2002).
18. Boucher, O. & Haywood, J. On summing the components of radiative forcing of climate change, *Clim. Dyn.*, 18, 297-302 (2001).
19. Dubovik, O. *et al.* Variability of absorption and optical properties of key aerosol types observed in worldwide locations. *J. Atmos. Sci.*, **59**, 590-608 (2002).

20. Cox, C. & Munk W. Statistics of the sea surface derived from sun glitter. *J. Mar. Res.* **13**, 198-227 (1954).

**Acknowledgements** We thank Bertrand Crouzille for helping with the processing of MODIS data.

**Competing interests statement** The authors declare that they have no competing financial interests.

**Correspondence** and requests for materials should be addressed to N.B. (nicolas.bellouin@metoffice.gov.uk).